ACS APPLIED MATERIALS & INTERFACES

Research Article

Cite This: ACS Appl. Mater. Interfaces 2019, 11, 36399−36408

www.acsami.org

"Three-in-One" SERS Adhesive Tape for Rapid Sampling, Release, and Detection of Wound Infectious Pathogens

Jingxing Guo,[†] Zhihao Zhong,[†] Yumei Li,[‡] Ying Liu,*[,†] Ruiyong Wang,*[,‡] and Huangxian Ju*[,†]

[†]State Key Laboratory of Analytical Chemistry for Life Science, School of Chemistry and Chemical Engineering, and [‡]State Key Laboratory of Pharmaceutical Biotechnology, School of Life Sciences, Nanjing University, Nanjing 210023, P. R. China

Supporting Information

ABSTRACT: The traditional colony culture method for detection of pathogens is subjected to the laborious and tedious experimental procedure, which limits its application in point-of-care (POC) testing and quick diagnosis. This work designs an intelligent adhesive tape as a "three-in-one" platform for rapid sampling, photocontrolled release, and surface-enhanced Raman scattering (SERS) detection of pathogens from infected wounds. This tape is constructed by encapsulating densely packed gold nanostars as SERS substrates between two pieces of graphene and modified with a synthetic *o*-nitrobenzyl derivative molecule to form an artificial biointerface for highly efficient pathogen capture via electrostatic interaction. The captured targets can be conveniently released onto a solid culture medium by UV cleavage of *o*-nitrobenzyl moiety for pathogen growth and in situ SERS detection. As a proof of strategy, this "three-in-one" platform has been used for detecting the concurrent infection of *Pseudomonas aeruginosa* and *Staphylococcus aureus* by pasting the tape on a skin burn wound. The impressive detection performance with an analytical time of only several hours for these pathogens at an early growth stage demonstrates its great potential as a POC testing device for health care.

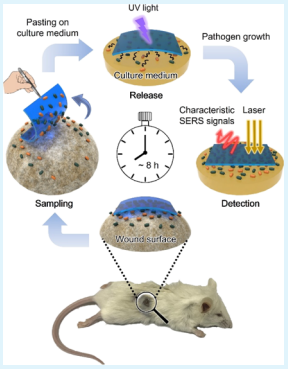

KEYWORDS: *pathogen capture and release, pathogen detection, photoresponsive, soft biosensor, surface-enhanced Raman scattering*

Bacterial infectious disease is one of the greatest global challenges in human health care.[1] Wound infection, which is caused by the invasion of pathogenic microorganisms through skin, can impede the healing process and lead to life-threatening complications.[2] Thus, the rapid and sensitive detection of wound infectious pathogens at their early stage is crucial to antimicrobial treatment. The clinical gold standard for pathogen detection generally uses the colony culture method, which includes pathogen collection and transfer, long-term culture in multiple media, morphological analysis, and immunoassays of pathogen metabolites.[3,4] However, the laborious, tedious, and complex experimental procedure limits its application in point-of-care (POC) testing and quick diagnosis. There is still an urgent demand for an efficient platform that integrates pathogen sampling from skin wound, controlled release for pathogen growth, and sensitive and specific detection of wound infectious pathogens.

The efficient sampling and transfer of pathogens from routine screening samples to culture media are essential steps in pathogen detection. Several conventional strategies such as immune magnetic beads[5,6] and microfluidics[7,8] have been proposed for pathogen collection, but the tedious operation processes limit their applications in POC testing. Therefore, some artificial biointerfaces have been developed for controllable pathogen capture and/or release by using phenylboronic acid-, mannose-, and cyclodextrin-functionalized platforms.[9−12] However, it is difficult to use these rigid devices for pathogen sampling on wound surface because of the low pathogen capture efficiency from insufficient contact between the rigid platform and the uneven samples. In order to improve the contact and capture efficiency, it is necessary to use soft materials such as carbon nanotubes, cellulose paper, polyester films, and nanobrush borders[13−15] to construct the "smart" biointerfaces for capture and release of pathogens. These developed devices show their potential in elimination of pathogens and POC diagnostic assays. Considering the good biocompatibility[16] and outstanding capability of graphene to improve the surface-enhanced Raman scattering (SERS) signal,[17] here we used single-layer graphene (1LG) as a flexible material to design a pathogen capture adhesive tape for highly efficient sampling. Through modifying a photoresponsive molecule on the surface of the tape , both the pathogen sampling by the electrostatic interaction[18,19] and the photocontrolled release and transfer of the captured pathogens were achieved.

To integrate the controlled pathogen sampling and release ability of the designed adhesive tape with signal extraction, the photocontrolled adhesive tape was constructed by wrapping densely packed multi-sized gold nanostars (mAuNSs) between two pieces of 1LG, implanting 4-mercaptobenzoic acid (4-MBA) as an internal standard (IS) on the top of 1LG for SERS detection,[20,21] and modifying the synthetic UV-photocleavable (PC) molecule on the bottom of 1LG (Scheme 1a). The constructed SERS adhesive tape could be directly pasted on

Received: July 21, 2019
Accepted: September 11, 2019
Published: September 11, 2019

DOI: 10.1021/acsami.9b12823
ACS Appl. Mater. Interfaces 2019, 11, 36399−36408

Scheme 1. Schematic Illustration of (a) SERS Adhesive Tape for Pathogen Capture and Release and (b) Pathogen Sampling from Skin Wound, Photocontrolled Release to Solid Culture Medium for Pathogen Growth, and in Situ SERS Detection

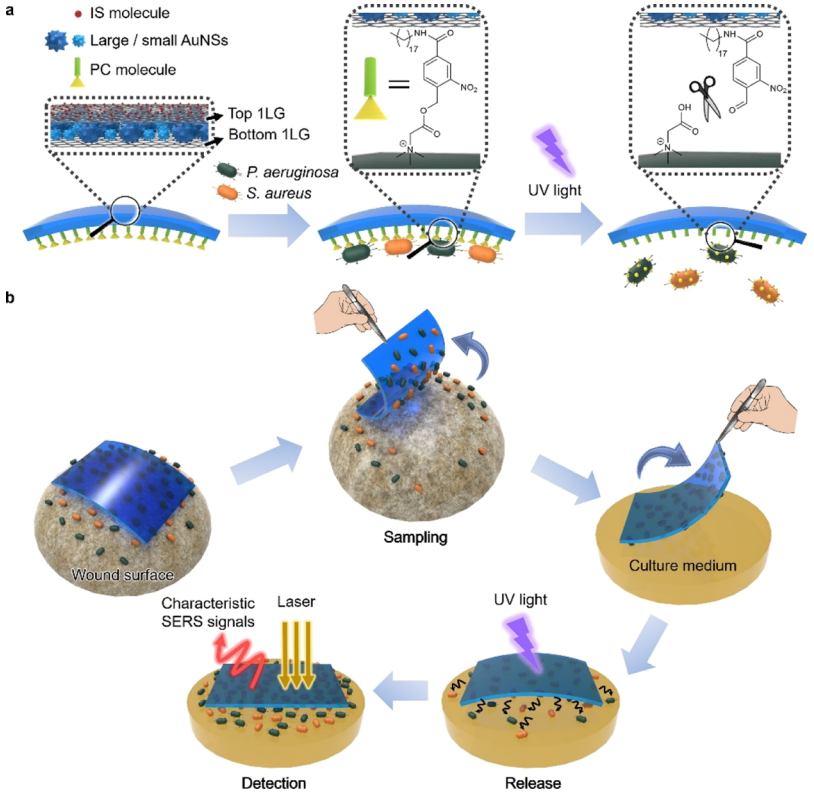

the surface of skin wound for pathogen sampling. After the captured pathogens were released onto a solid culture medium by UV cleavage of *o*-nitrobenzyl moiety for efficient pathogen growth, the in situ SERS detection of pathogens could be performed via collecting the characteristic SERS signals (Scheme 1b). Taking *Pseudomonas aeruginosa* and *Staphylococcus aureus* as model analytes, which are the common wound infectious pathogens to cause sepsis[22,23] and the potential dominant species in burn-injured wounds, we demonstrated the ability of this "three-in-one" platform for simultaneous detection of two pathogens at an early growth stage, which were sampled from an infected skin burn wound. The whole analytical time from sampling to detection was much lesser than the current clinic methods. The specific detection and local distribution imaging of two model pathogens indicated the great potential of the intelligent adhesive tape as a POC testing device for rapid detection of bacterial infection types, which may offer guidance to antibiotic treatments.

EXPERIMENTAL SECTION

Materials and Reagents. Polymethyl methacrylate (PMMA) (2% wt in ethyl lactate) was from Alresist (Germany). 1LG prepared on a Cu foil by chemical vapor deposition was obtained from ACS Materials (USA). Triethylamine (Et_3N) (≥99%), dodecanethiol (DDT) (≥98%), chloroauric acid ($HAuCl_4{\cdot}3H_2O$) (99%), polyvinylpyrrolidone (PVP, MW = 10 000), 4-MBA (99%), 6-carboxyfluorescein (6-FAM) (99%), pyocyanin (≥98%), and propidium iodide (PI) (≥94%) were from Sigma-Aldrich Inc. (USA). Stearylamine (≥98%) and 4-(4,6-dimethoxy-1,3,5-triazin-2-yl)-4-methylmorpholinium chloride (DMT-MM) (>98%) were purchased from Tokyo Chemical Industry Co., Ltd. (Tokyo, Japan). Acetonitrile (99.9%), 4-bromonethyl-3-nitrobenzoic acid (97%), and methyl alcohol (MeOH) (99.9%) were from J&K Scientific Ltd. (Beijing, China). Betaine (≥98%), thionylchloride ($SOCl_2$) (≥99%), and ethyl lactate (99%) were from Adamas-beta (China). Acetone (99.5%), Na_2CO_3 (≥99.8%), and NaOH (≥96%) were from Nanjing Chemical Reagent Co., Ltd. (China). Ethanol (≥99.7%), *N*,*N*-dimethylformamide (DMF, ≥ 99.8%), trisodium citrate (≥99%), HCl (37% in water), and $FeCl_3{\cdot}6H_2O$ (99%) were obtained from Sinopharm Chemical Reagent Co., Ltd. (China). Glutaraldehyde (50% in water) was purchased from Energy Chemical Co., Ltd. (China). The Luria–Bertani (LB) medium was prepared by dissolving the LB broth (containing 10 g of tryptone, 5 g of yeast extract, and 10 g of NaCl) in 1 L of water and then autoclaving. LB plates were obtained by mixing 25 g of LB broth and 15 g of agar (Sangon Biological Engineering Technology Co., Ltd., China) to dissolve in 1 L of water for autoclaving and then cooling to room temperature. 1× Phosphate-buffered saline (PBS) (pH 7.4, 0.1 μm sterile-filtered) was purchased from HyClone (USA). *P. aeruginosa* (wild type, ATCC9027) and *S. aureus* (wild type, ATCC6538P) were obtained from the National Center for Medical Culture Collections (CMCC, China). The SYTO 9 green fluorescent nucleic acid stain (5 mM in dimethyl sulfoxide) was obtained from Thermo Fisher Scientific (USA). Depilatory cream (Veet, France) was obtained from a local supermarket. Male BALB/c mice (Specific Pathogen Free) at an age of 7 weeks were purchased from the Model Animal Research Center of Nanjing University (MARC, China). All solutions were prepared using ultrapure water (18 MΩ, Milli-Q, Millipore).

Apparatus. Transmission electron microscopy (TEM) and scanning electron microscopy (SEM) images were obtained on a JEM-2100 transmission electron microscope (JEOL, Japan) and a S-4800 scanning electron microscope (Hitachi, Japan), and the sputtering deposition of pathogen samples was performed on a SCD 500 sputter coater (Bal-Tec, USA). The TEM images were analyzed with ImageJ software. The fabrication of AuNSs@1LG foil was performed on a TMS-300 temperature-controlled vibrator (Hangzhou Allsheng Instruments Co., Ltd., China). Spin-coating and drying of PMMA were performed on a spin coater and a hot plate

DOI: 10.1021/acsami.9b12823
ACS Appl. Mater. Interfaces 2019, 11, 36399−36408

(SETCAS Electronics Co., Ltd., China), respectively. The nuclear magnetic resonance (NMR) spectra were obtained from AVANCE III 500 (Bruker, Germany), and the electron spray ionization mass spectroscopy (ESI-MS) spectra were obtained from LTQ-Orbitrap XL (Thermo Fisher, USA). The UV−vis absorption spectra and the Fourier transform infrared (FTIR) spectra were recorded on a UV-3600 UV−Vis−NIR spectrophotometer (Shimadzu, Japan) and a VERTEX80V vacuum FTIR spectrometer (Bruker, Germany), respectively. Dynamic light scattering and zeta potential measurements were performed on a 90 Plus/BI-MAS instrument (Brook Haven, USA). The contact angle measurements were carried out on an OCA30 contact angle meter (DataPhysics, Germany). The fluorescence spectra were obtained from a FluoroMax-4 spectrofluorometer (Horiba, Japan), and fluorescence imaging was performed on a TCS SP5 laser scanning confocal microscope (Leica, Germany). Raman spectra were recorded on a Renishaw inVia confocal Raman microscope (Renishaw, UK), and the 50× telephoto objective with a numerical aperture of 0.5 was used for optical images and spectral measurements. All the data were analyzed with WiRE 3.4 and Origin 8.0 software. UV irradiation was performed by a USB charging UV flashlight (Shenzhen Langheng Electronics Co., Ltd., China). The pathogen culture was carried out in a thermostatic oscillator (Jintan Science Analysis Instrument Co., Ltd., China) for an LB medium or in a humidified chamber (Shanghai CIMO Medical Instrument Manufacturing Co., Ltd., China) for an LB agar plate.

Synthesis of the PC Molecule. The PC molecule **6** (*N,N,N*-trimethyl-2-((2-nitro-4-(octadecylcarbamoyl)benzyl)oxy)-2-oxoethan-1-aminium) was synthesized according to Scheme S1a. 2-Chloro-*N,N,N*-trimethyl-2-oxoethan-1-aminium chloride (**2**) was first prepared according to previous procedures.[24] Briefly, 2.0 g of (carboxymethyl)trimethylammonium hydrochloride (**1**) (1.3 mmol) was suspended in 30 mL (0.41 mol) of thionyl chloride in a round-bottom flask. The reaction system was heated at 60 °C for 1 h. After the emission of sulfur dioxide was ceased, excess thionyl chloride was removed by evaporation under reduced pressure. The product was washed thrice with 100 mL of *n*-hexane and decanted for removal of the solvent. The crude product was dried in vacuum to obtain 1.8 g of **2**.

4-(Hydroxymethyl)-3-nitrobenzoic acid (**4**) was prepared as reported previously.[25] Briefly, a mixture of 4-(bromomethyl)-3-nitrobenzoic acid (**3**) (3.5 g, 13.5 mmol) and sodium carbonate (7.8 g, 74.3 mmol) in acetone−water (50 mL, 1:1) was heated under reflux for 5 h. The mixture was cooled to room temperature and acetone was then evaporated. The resulting aqueous phase was acidified to pH 1 with 1 M HCl, extracted with ethyl acetate (50 mL × 3), dried over $MgSO_4$, and concentrated in vacuo to yield 2.5 g (95%) of **4**.

4-(Hydroxymethyl)-3-nitro-*N*-octadecylbenzamide (**5**) was synthesized as follows: 0.88 g of DMT-MM (3.0 mmol), 0.65 g of octadecylamine (2.4 mmol), and 0.39 g of **4** (2.0 mmol) were mixed in 20 mL of methanol and allowed to stir overnight at room temperature. After the solvent was removed by evaporation under reduced pressure, the residue was purified by column chromatography on silica gel with eluent EA/PE (1:2) to obtain **5**.

The PC molecule **6** was synthesized as follows: 0.14 g of **2** (0.8 mmol) and 0.32 g of **5** (0.88 mmol) were mixed in an anhydrous acetonitrile solvent (10 mL). The reaction mixture was heated up to 50 °C and stirred for 6 h. Then, the mixture was cooled to room temperature. After the removal of the precipitate from the bottom, the solvent of the supernatant was removed under reduced pressure. The crude product was purified by recrystallization in acetonitrile solvent and the final product **6** was obtained. ^{1}H NMR (500 MHz, DMSO): δ 8.85 (t, J = 5.0, 1H), 8.62 (d, J = 1.6, 1H), 8.26 (dd, J = 8.1, 1.7, 1H), 7.85 (d, J = 8.1, 1H), 5.66 (s, 2H), 4.60 (s, 2H), 3.29 (m, 2H), 3.26 (s, 9H), 1.54 (m, 2H), 1.26 (m, 30H), 0.86 (t, J = 6.9, 3H) (Figure S1). ^{13}C NMR (125 MHz, DMSO): δ 164.95, 163.87, 147.55, 133.45, 132.96, 130.18, 124.09, 64.22, 63.00, 53.73, 29.48, 29.21, 29.16, 26.92, 22.56, 14.43 (Figure S2). HRMS-ESI (m/z): $[M - Cl]^+$ calcd for $C_{31}H_{54}N_3O_2^+$, 548.4058; found, 548.4111 (Figure S3).

The control molecule **7** was synthesized according to Scheme S1b: 0.17 g of 2 (1.0 mmol) and 0.22 g of octadecylamine (0.8 mmol) were mixed in an anhydrous acetonitrile solvent (10 mL). The reaction mixture was heated up to 50 °C and then 138 μL of trimethylamine (1.0 mmol) was injected. After stirring overnight, the mixture was cooled to room temperature. After the removal of the precipitate from the bottom, the solvent of the supernatant was removed under reduced pressure. The crude product was purified by recrystallization in acetonitrile solvent and the final product of trimethyl-2-(octadecylamino)-2-oxoethan-1-aminium chloride (**7**) was obtained. ^{1}H NMR (500 MHz, DMSO): δ 8.61 (s, 1H), 4.09 (s, 2H), 3.21 (s, 9H), 3.13−3.05 (m, 2H), 1.33−1.11 (m, 32H), 0.86 (t, J = 6.9, 3H) (Figure S4). ^{13}C NMR (125 MHz, DMSO): δ 166.86, 63.01, 53.37, 32.70, 31.76, 29.50, 29.46, 29.17, 29.14, 22.56, 14.44 (Figure S5). HRMS-ESI (m/z): $[M - Cl]^+$ calcd for $C_{23}H_{49}N_2O^+$, 369.3839; found, 369.3905 (Figure S6).

Synthesis of AuNSs. The synthesis of small AuNSs (sAuNSs) and large AuNSs (lAuNSs) was carried out according to our previously reported method.[20] First, PVP-coated gold seeds (15 nm in diameter) were prepared by rapidly adding 5 mL of trisodium citrate (1% wt) into 100 mL of boiling $HAuCl_4$ solution (0.5 mM) to react for 15 min. After the mixture was cooled to room temperature, 8.6 mL of PVP (25.6 g/L, MW = 10 000) was added dropwise and allowed to stand overnight. The resulting gold seeds were sedimentated by centrifugation (4000 rpm, 90 min) and redispersed in 4 mL of ethanol. The AuNSs were then synthesized by adding 301 μL of as-prepared gold seeds (4.2 mM) into 105 mL of DMF solution containing PVP (10 mM) and 0.3 mM (for sAuNSs) or 1.2 mM (for lAuNSs) $HAuCl_4$ under rapid stirring for 15 min. The resulting sAuNSs and lAuNSs were washed by centrifugation (10 000 or 6000 rpm, 10 min, respectively) and redispersed in ethanol.

Fabrication of SERS Adhesive Tape. One piece of 1LG foil was cut into a suitable size (4.5 × 4.5 mm in this work), cleaned with nitrogen flow, and vertically immersed into the 1 mM DDT ethanol solution for 1 h under room temperature. After rinsing with water and drying by nitrogen flow, the 1LG foil was vertically immersed into the ethanol solution of 1 nM lAuNSs and incubated under 43 °C and 350 rpm for 18 h. After rinsing with water and drying by nitrogen flow, the lAuNS-assembled 1LG foil was vertically immersed into the ethanol solution of 1 nM sAuNS and incubated under 43 °C and 350 rpm for 18 h. After rinsing with water and drying by nitrogen flow, the mAuNSs@1LG foil was obtained.

Another piece of 1LG foil was cut into a slightly smaller size (4.0 × 4.0 mm in this work) than the mAuNSs@1LG foil, cleaned with nitrogen flow, and vertically immersed into a 10 mM ethanol solution of MBA as an IS for 1 h under room temperature. It was then gently rinsed with water and dried by nitrogen flow to obtain the IS@1LG foil, and 1 wt % PMMA in ethyl lactate was subsequently spin-coated (2000 rpm, 60 s) on the IS side of the IS@1LG foil. After drying the PMMA coating on a hot plate at 120 °C for 5 min, the Cu substrate was etched in 1.0 M $FeCl_3$. The obtained IS-implanted 1LG membrane was then rinsed with 1:4 HCl and water and transferred onto the top of the mAuNSs@1LG foil to form a sandwich-type IS-1LG@mAuNS@1LG foil. After air-drying and then spin-coating 2 wt % PMMA in ethyl lactate (4000 rpm, 60 s) to dry on a hot plate at 120 °C for 5 min, the Cu substrate was etched in 1.0 M $FeCl_3$ to obtain an IS-1LG@mAuNS@1LG slice, which was immersed in the ethanol solution of 1 mM PC molecule **6** for 1 min to obtain the SERS adhesive tape. The control SERS adhesive tape was obtained by immersing the IS-1LG@mAuNS@1LG slice in the ethanol solution of 1 mM control molecule **7** for 1 min.

Raman Characterization of SERS Tape. The signal uniformity and photostability of the SERS tape were evaluated with the SERS signal of 4-MBA, which was obtained from the tape held on a silicon wafer under 785 nm with a 50× telephoto objective, an exposure time of 1 s, and a laser power of 4.5 mW. The SERS imaging area was 100 μm × 100 μm, and the data were collected using the signal-to-baseline map review mode from 1056 to 1100 cm^{-1} for 4-MBA. The relative standard deviation (RSD) and average signal intensity were calculated from 441 collection points in each imaging graph. The SERS

DOI: 10.1021/acsami.9b12823
ACS Appl. Mater. Interfaces 2019, 11, 36399−36408

responses to pyocyanin standard solutions were recorded by floating the tape on different concentrations under 785 nm with a 50× telephoto objective, an exposure time of 10 s, and a laser power of 4.5 mW. The power density used for Raman measurements was 1.6 mW/μm^2, which was calculated from the laser power and area of the laser spot.

Photocleavage Efficiency. The photocleavage efficiency of the adhesive tape was evaluated with a negatively charged fluorescence molecule, 6-FAM. First, 1 μM 6-FAM sodium was obtained by mixing equimolar 6-FAM and NaOH, and its fluorescence intensity at 518 nm excited by 492 nm was measured as I_0. Next, one piece of the adhesive tape was floated on the 6-FAM sodium solution and then gently vibrated for 5 min to capture 6-FAM, and the fluorescence intensity of the solution was measured as I_a. Finally, the 6-FAM-adsorbed adhesive tape was transferred to pure water after rinsing, followed by UV flashlight irradiation for 2 min, and then rinsed through repeatedly blowing with a pipette. The fluorescence intensity of the water-containing released 6-FAM was measured as I_b. Considering the fluorescence intensity proportional to the mole number of 6-FAM, the released efficiency was calculated according to the following eq 1

$$\text{Photocleavage efficiency (\%)} = \frac{I_b}{I_0 - I_a} \times 100\% \quad (1)$$

The mean value of the photocleavage efficiency was obtained as 92.4 ± 4.0% from five parallel experiments. Furthermore, the control experiment was also carried out with similar processes except for replacing UV irradiation with continuous shaking.

Pathogen Capture Efficiency. *P. aeruginosa* and *S. aureus* obtained from CMCC were first dispersed into the LB medium and incubated overnight at 37 °C with agitation (220 rpm). Then, the pathogens were inoculated by an inoculating loop into the LB medium of 10 mL and grown at 37 °C with agitation (220 rpm) for 10 h. Afterward, the pathogens at the exponential growth phase were collected and washed three times by centrifugation (8000*g* for 3 min) with 1× PBS, and the cell pellets were resuspended in LB medium for further use. The number of pathogens was determined by standard colony counting method as cfu values.

In order to assess the pathogen capture ability, the adhesive tape was first pasted on a cover glass with the PC-modified side facing up. Then, the glass was immersed into a 1 × 10^8 cfu/mL pathogen suspension with gentle vibration for 5 min to capture the pathogens. The pathogen density on the tape was calculated using eq 2

$$\text{Pathogen density (cm}^{-2}) = \frac{N_{total} - N_{rest}}{s} \quad (2)$$

where N_{total} and N_{rest} are the number of pathogens in the solution before and after capture, respectively, which were determined using the standard colony counting method, and s is the area of the adhesive tape. Furthermore, the control experiment was also carried out with similar processes except for replacing the SERS adhesive tape with silicon and the SERS tape without PC-modification.

The capture was carried out at a low pathogen concentration with similar processes except for changing the concentration of pathogen suspension to 100, 500, or 1000 cfu/mL and the vibration time to 60 min. The capture efficiency was calculated using eq 3

$$\text{Capture efficiency (\%)} = \left(\frac{N_{total} - N_{rest}}{N_{total}}\right) \times 100\% \quad (3)$$

where N_{total} and N_{rest} are the number of pathogens in the solution before and after capture, respectively, which are determined using the standard colony counting method.

SEM Imaging of Captured Pathogens. The adhesive tape was held on a silicon wafer after pathogen capture, and then the wafer was rinsed by water and air-dried, incubated in 1× PBS containing 2.5% glutaraldehyde for 45 min at 4 °C, and rinsed with 1× PBS and water. The pathogens were subsequently dehydrated by sequentially immersing the wafer in 30, 50, 70, and 90% ethanol for 5 min and anhydrous ethanol for 10 min. The wafer was air-dried followed by sputtering deposition of 8 nm gold layer to take the SEM image using an accelerating voltage of 5 keV.

Release Efficiency of Captured Pathogens. After the pathogen capture process, the surface of the adhesive tape was gently rinsed with water and the tape was immersed into 20 μM SYTO 9 solution. After standing in the dark for 30 min, the sample was gently rinsed with water and air-dried, and the pathogens captured by the adhesive tape were imaged using a confocal fluorescence microscope equipped with a 100× oil-immersed objective under 488 nm excitation. The average number of pathogens captured by the adhesive tape ($N_{capture}$) was determined from the fluorescence image. The average number of pathogens remained on the adhesive tape after UV irradiation for 2 min ($N_{residual}$) was also determined in the same way. The pathogen release efficiency was calculated using eq 4

$$\text{Release efficiency (\%)} = \left(\frac{N_{capture} - N_{residual}}{N_{capture}}\right) \times 100\% \quad (4)$$

Viability of Captured and Released Pathogens. SYTO 9/PI stains were used to evaluate the viability of pathogens captured on the adhesive tape. Live pathogens with intact cell membranes were stained by SYTO 9, whereas dead pathogens with damaged membranes were stained by PI. Specifically, after the pathogen capture process, the surface of the adhesive tape was gently rinsed by water and the tape was immersed into the SYTO 9/PI mixture (containing 5 μM SYTO 9 and 30 μM PI). After standing in the dark for 30 min, the sample was gently rinsed by water and air-dried, and the sample was imaged using a confocal fluorescence microscope equipped with a 100× oil-immersed objective under 488 nm excitation for SYTO 9 and 535 nm excitation for PI. The reproduction activity of released pathogens was detected by monitoring the absorbance of their cultured LB medium at 600 nm.

Mouse Model of Skin Burn Wound. The model of skin burn wound was set up according to previous literature studies.[26,27] First, one mouse was anesthetized and sterilized by 70% ethanol. Then, a proper amount of depilatory cream was smeared to the back of the mouse to expose the skin. A lighted cigarette butt was made to touch the skin for 5 s and burn a round wound with a diameter of around 7 mm. After the burn wound was rinsed and sterilized, the mouse model was ready for spiking with a pathogen suspension. All mice were euthanized after pathogen sampling.

All animal protocols were reviewed and approved by the Animal Care and Use Committee of Nanjing University. Mice were fed in a specific pathogen-free animal facility with controlled light (12 h light/dark), temperature, and humidity, with food and water available.

Sampling, Release, and Detection of Pathogens from the Infected Surface. The sampling of pathogens was first performed from the LB agar surface. After the 1 × 10^8 cfu/mL pathogen suspension (*P. aeruginosa* or *S. aureus*) was smeared on the LB agar surface and air-dried, one piece of adhesive tape was taken out from water and pasted on the pathogen-infected area with a tweezer. The adhesive tape was then torn off, rinsed with water, and pasted on a new sterile LB agar, followed by UV irradiation for 2 min, and placed in a humidified chamber at 37 °C for pathogen growth. The SERS spectra were collected under 785 nm with an exposure time of 10 s and a laser power of 4.5 mW. The SERS imaging area with 50× telephoto objective was 100 μm × 100 μm, and data were collected using the signal-to-baseline map review mode from 1056 to 1100 cm^{-1} for 4-MBA and 1330 to 1382 cm^{-1} for *P. aeruginosa* or 1100 to 1144 cm^{-1} for *S. aureus* under 785 nm with an exposure time of 1 s and a laser power of 4.5 mW. The power density used for Raman measurements was 1.6 mW/μm^2. In addition, the nether pathogen number was measured as follows: after 4 h of pathogen growth, the adhesive tapes were torn off and inoculating loops were used to collect the nether pathogens, followed by immersing into 1 mL of 1× PBS, and the live pathogen number could be counted with the standard colony counting method.

For detecting the concurrent infection model on a mouse burn wound, a 1 × 10^6 cfu/mL pathogen mixture containing equal

DOI: 10.1021/acsami.9b12823
ACS Appl. Mater. Interfaces 2019, 11, 36399−36408

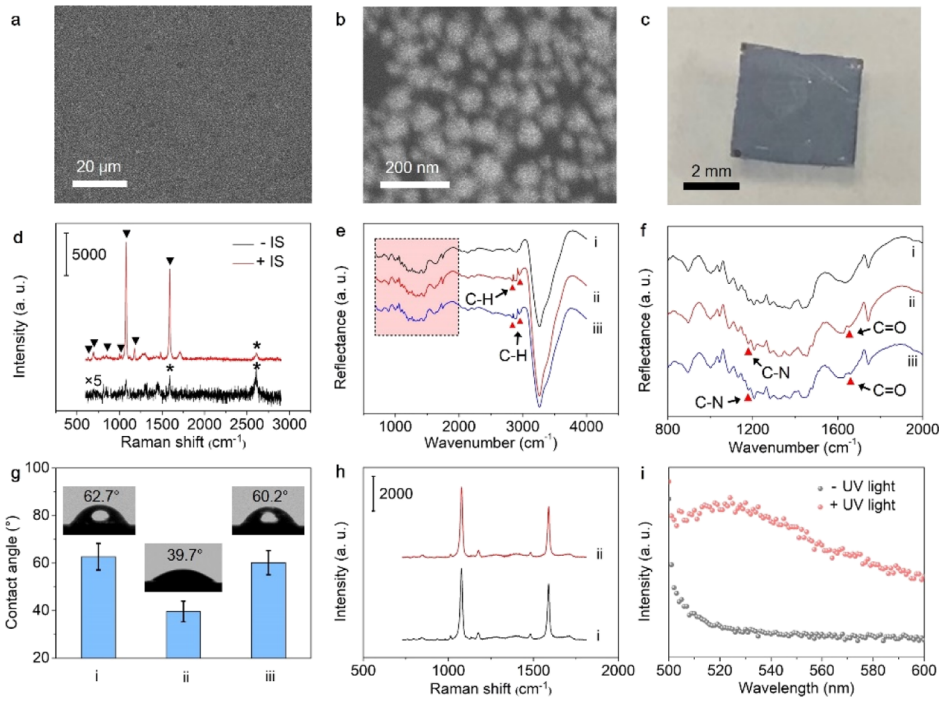

Figure 1. Characterization of SERS tape. (a,b) SEM and (c) optical images, and (d) SERS spectra of SERS tape in the presence and absence of IS. The marks indicate the characteristic SERS peaks of IS and 1LG. (e) FTIR spectra of SERS tape without (i) and with PC molecule modification before (ii) and after (iii) UV irradiation. (f) Magnification of the pink box in (e). The marks indicate the characteristic peaks of the PC molecule. (g) Contact angles of SERS tape without (i) and with PC molecule modification before (ii) and after (iii) UV irradiation (n = 5). (h) SERS spectra of SERS tape without (i) and with (ii) PC molecule modification. (i) Fluorescence intensity of 6-FAM released from the adhesive tape without or with UV irradiation. Excitation laser: 785 nm; laser power: 4.5 mW; and exposure time: 10 s.

proportion of *P. aeruginosa* and *S. aureus* was smeared on the sterilized surface and air-dried, and one piece of adhesive tape was pasted on the pathogen-infected area with a tweezer. After the adhesive tape was torn off and rinsed with water, it was pasted on a sterile LB agar to perform UV irradiation for 2 min and then placed in a humidified chamber at 37 °C for 8 h. The SERS spectra were collected under 785 nm with an exposure time of 10 s and a laser power of 4.5 mW. The SERS imaging area with 50× telephoto objective was 100 μm × 100 μm, and the data were collected using the signal-to-baseline map review mode from 1056 to 1100 cm^{-1} for 4-MBA and 1330 to 1382 cm^{-1} for *P. aeruginosa* or 1100 to 1144 cm^{-1} for *S. aureus* under 785 nm with an exposure time of 1 s and a laser power of 4.5 mW. The power density used for Raman measurements was 1.6 mW/μm^2.

RESULTS AND DISCUSSION

Preparation and Characterization of the SERS Adhesive Tape. Two different sizes of AuNSs were synthesized for the preparation of the SERS adhesive tape by self-assembling them on the 1LG surface, which could form a denser monolayer of AuNSs and bring stronger SERS signal than the layer of single-sized gold nanostars.[20] These AuNSs showed the core radii of 39.7 ± 5.4 and 21.7 ± 4.2 nm and hydrodynamic diameters of 126.0 ± 39.2 and 91.0 ± 19.6 nm, respectively (Figure S7). The lAuNSs showed an absorbance peak at 792 nm, while the absorbance peak of sAuNSs occurred at 749 nm (Figure S8); thus, they could produce strong SERS effect under the laser irradiation of 785 nm.[28] After the mAuNSs were densely packed between two 1LG layers with uniform distribution (Figure 1a,b) and the IS was implanted on the top layer, the prepared SERS tape showed uniform dark blue color (Figure 1c), two characteristic SERS peaks of 1LG at 1589 and 2610 cm^{-1},[29] and a series of SERS peaks of IS at 631, 693, 847, 1013, 1076, 1178, and 1591 cm^{-1}[30,31] (Figure 1d). The signals of IS represented acceptable uniformity and reproducibility in 100 μm × 100 μm area, which showed the RSD of 10.2, 10.7, and 10.3% with similar signal intensities from the tapes fabricated in three different days (Figure S9a–d). The SERS tape was also stable against laser irradiation with 4.1% RSD signal fluctuation under continuous irradiation for 600 s (Figure S9e,f). The impressive SERS uniformity, reproducibility, and stability guaranteed the high-quality SERS measurements.

The PC molecule consisted of three functional parts: a long alkane chain for 1LG anchoring,[32] an *o*-nitrobenzyl moiety for UV-responsive cleavage, and a quaternary ammonium group for pathogen capturing (Scheme S1a). After the SERS tape was modified with a PC molecule, its FTIR spectrum showed four new peaks at 1180, 1653, 2840, and 2948 cm^{-1} (Figure 1e,f), which were assigned to the C−N stretching vibration of quaternary ammonium group, C═O stretching vibration of amide group, and C−H stretching vibration of methylene and methyl, respectively.[33] Upon 365 nm irradiation, the characteristic peak at 1180 cm^{-1} became weaker (curve iii, Figure 1f), indicating the effective photocleavage of the PC molecule. The PC molecule modification decreased the contact angle from 62.7° to 39.7°, which then increased to 60.7° upon UV irradiation (Figure 1g), close to the contact angle in the absence of PC molecule (Figure S10), indicating the presence and photoresponsive cleavage of quaternary ammonium ion. It should be pointed out that the PC molecule modification did not bring extra SERS peak in the range of 700−1800 cm^{-1} because of the overlap of characteristic peaks of PC and IS molecules (Figure 1h). Although the adhesive tape showed the strengthened C−H stretching peaks of methylene at 2848 cm^{-1} and methyl at 2925 cm^{-1} in the presence of PC molecule,

DOI: 10.1021/acsami.9b12823
ACS Appl. Mater. Interfaces 2019, 11, 36399−36408

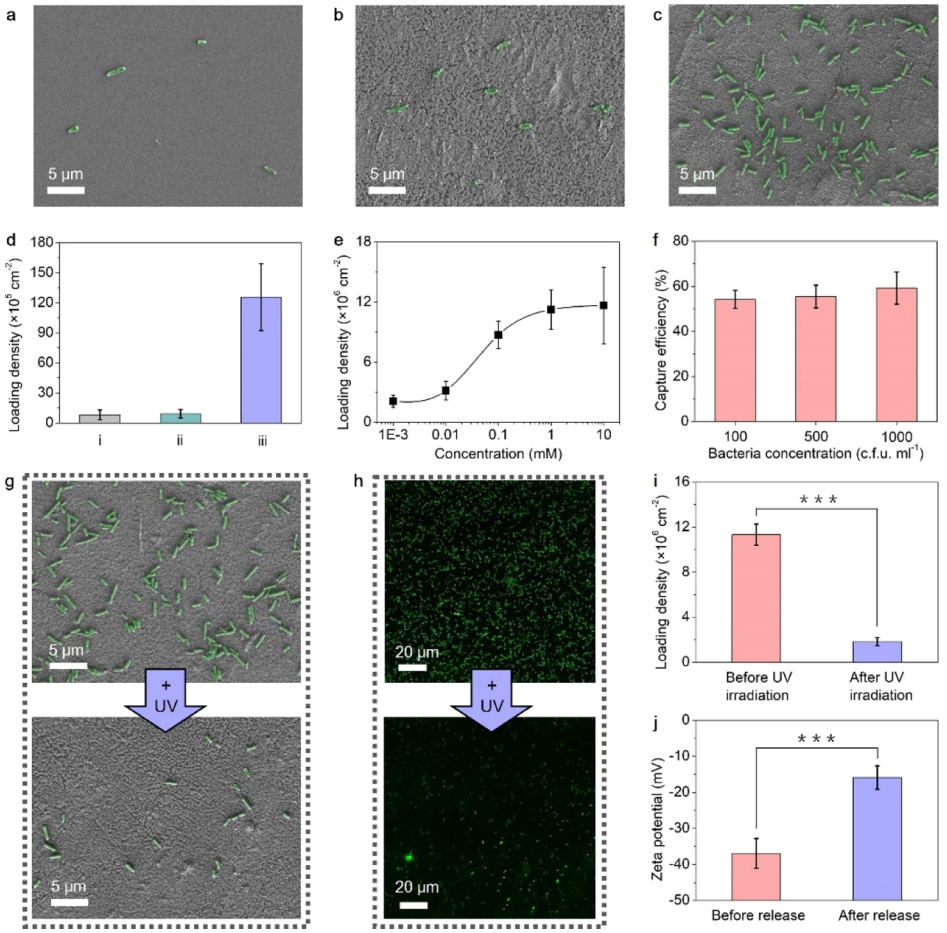

Figure 2. Pathogen capture and photoresponsive release. SEM images of *P. aeruginosa* captured on silicon wafer (a), and SERS tape without (b) and with (c) PC molecule modification. (d) Corresponding loading density. (e) Loading densities on the tape modified with different concentrations of PC molecule. (f) Capture efficiency at 100, 500, and 1000 cfu/mL of pathogen. (g) SEM and (h) confocal fluorescence images of *P. aeruginosa* captured on adhesive tape before and after UV irradiation. (i) Corresponding loading densities. ***$P < 0.001$ determined by two-tailed Student's *t*-test. (j) Zeta potentials of original and photoreleased *P. aeruginosa*. The data error bars indicate means ± SD ($n = 10$ for d–f and i, and $n = 5$ for j).

these peaks did not interfere with the SERS detection of pathogens (Figure S11).

The photocleavage efficiency could be evaluated with a negative-charged fluorescence molecule, 6-FAM, which was first adsorbed on the adhesive tape via electrostatistic interaction. The UV irradiation led to obvious release of 6-FAM from the tape (Figure 1i). From the emission peak of released 6-FAM around 520 nm, the release efficiency for 2 min UV irradiation was measured up to 92.4 ± 4.0%, indicating that the tape owns the high photocleavage efficiency for rapidly releasing the negative-charged target.

Rapid Capture and Photoresponsive Release of Pathogens. After the adhesive tape was immersed in 1.0 × 10^8 cfu/mL of *P. aeruginosa* suspension for 5 min, the surface loading of *P. aeruginosa* reached 1.2 × 10^7 cm^{-2}, which was much higher than those obtained through nonspecific pathogen adsorption on silicon wafer (8.1 × 10^5 cm^{-2}) and the tape without PC molecule (9.2 × 10^5 cm^{-2}) (Figure 2a–d), as well as many previous reports.[10−12] Furthermore, the surface density of captured pathogens increased with the increasing amount of modified PC molecule and reached the maximum value as the tape prepared with 1 mM PC molecule (Figure 2e). The fluorescence images also demonstrated the same phenomenon (Figure S12), which confirmed that the PC molecule played an important role in pathogen capturing. The capture efficiency even in LB medium with low pathogen concentrations was measured as 54.2 ± 4.0, 55.5 ± 5.1, and 59.3 ± 7.2% for 100, 500, and 1000 cfu/mL *P. aeruginosa,* respectively (Figure 2f). More importantly, the captured *P. aeruginosa* showed good viability because of the excellent biocompatibility of the adhesive tape (Figure S13a–c).

To demonstrate the highly efficient photocontrolled release, the SERS adhesive tape was irradiated with a UV flashlight for only 2 min, which led to a sharp decrease of the surface density of *P. aeruginosa* to 83.9 ± 2.8% (Figure 2g–i). By contrast, the UV irradiation did not obviously change the surface density of *P. aeruginosa* captured on the control SERS adhesive tape (Figure S14) prepared with the control molecule, which has a similar structure to the PC molecule except the lack of *o*-nitrobenzyl moiety (Scheme S1b). Interestingly, the photo-released *P. aeruginosa* showed the zeta potential of −15.9 mV, more positive than −36.9 mV of original *P. aeruginosa* because of the presence of quaternary ammonium ions (Figure 2j). After the photocontrolled release, *P. aeruginosa* still retained good reproduction activity for its growth (Figure S13d).

Sampling, Release, and Detection of Pathogens from Infected LB-Agar. Because of the impressive pathogen capture and release capability, the soft SERS adhesive tape

DOI: 10.1021/acsami.9b12823
ACS Appl. Mater. Interfaces 2019, 11, 36399−36408

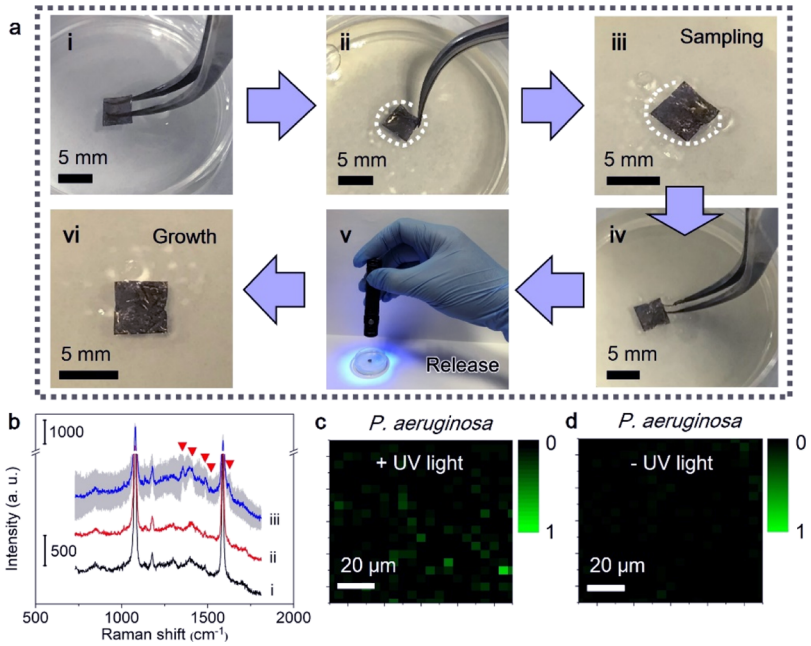

Figure 3. Sampling, release, and detection of *P. aeruginosa*. (a) Optical images of SERS detection processes: (i) taking SERS adhesive tape by a tweezer, (ii,iii) pasting the tape on *P. aeruginosa*-infected LB agar for sampling, (iv) tearing off and pasting the tape on a new sterile LB agar, (v) UV irradiating for 2 min, and (vi) pathogen growth to perform SERS detection. Dotted lines delineate the *P. aeruginosa* infected area. (b) Typical SERS spectra of adhesive tape pasted on LB agar (i), and *P. aeruginosa* sampled adhesive tape pasted on LB agar without (ii) and with (iii) UV treatment for 4 h growth. The light gray region indicates the SD (n = 60). (c,d) SERS imaging of b(iii) and b(ii). The red inverted triangles indicate the characteristic SERS peaks of *P. aeruginosa*. Excitation laser: 785 nm; laser power: 4.5 mW; and exposure time: 10 s for (b) and 1 s for (c,d).

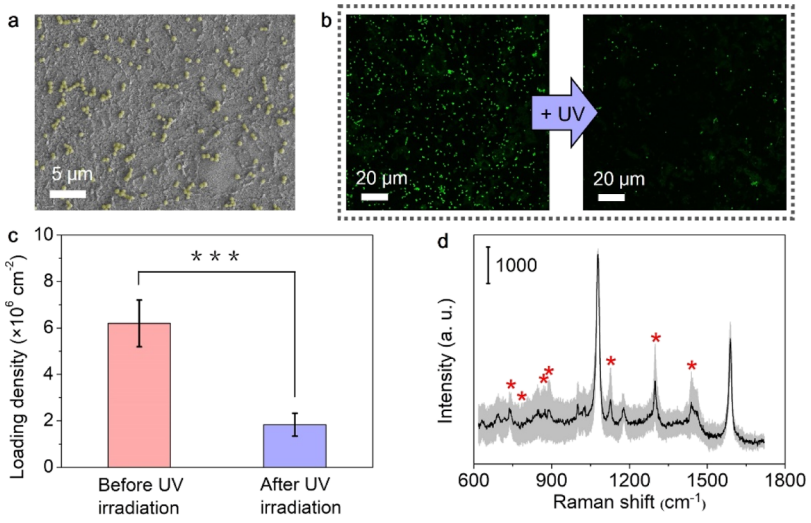

Figure 4. Sampling, release, and detection of *S. aureus*. (a) SEM image of *S. aureus* (yellow) captured on adhesive tape. (b) Confocal fluorescence images of *S. aureus* captured on adhesive tape before and after UV irradiation, and (c) corresponding average densities of *S. aureus*. The error bars indicate means ± SD (n = 10). ***P < 0.001 determined by two-tailed Student's t-test. (d) Typical SERS spectrum of adhesive tape after sampling from 1 × 10^8 cfu/mL of *S. aureus* contaminated LB agar, release, and 4 h growth. The light gray region indicates the SD (n = 60). The red asterisks indicate the characteristic SERS peaks of *S. aureus*. Excitation laser: 785 nm; laser power: 4.5 mW; and exposure time: 10 s.

could be used for pathogen sampling from solid objects and subsequent pathogen transfer onto a solid culture medium by photocontrolled release for pathogen growth and direct SERS signal extraction. As a proof of the "three-in-one" manner, a piece of SERS adhesive tape was pasted on a LB agar infected with 1 × 10^8 cfu/mL of *P. aeruginosa* for sampling and transfer of *P. aeruginosa* to sterile LB agar for growth (Figure 3a), which could be completed within 5 min. In order to detect *P. aeruginosa*, the pathogen growth time was optimized to be 4 h (Figure S15), at which *P. aeruginosa* was at its early growth stage (Figure S13d). Sixty SERS spectra were directly recorded on the adhesive tape and the mean spectrum is shown in Figure 3b. The reproducible SERS peaks at 1356 (ring stretching), 1408 (ring CH bending), 1486 and 1514 (CH_3 scissoring and ring CH bending), and 1622 cm^{-1} (ring stretching) were attributed to secreted pyocyanin as a biomarker,[28] and the intensity difference resulted from the inhomogeneous secretion of the *P. aeruginosa* biofilm. The tape demonstrated a detectable linear range of 2.0 × 10^{-9} to 1.0 × 10^{-6} M for spiked pure pyocyanin in aqueous solution with a

DOI: 10.1021/acsami.9b12823
ACS Appl. Mater. Interfaces 2019, 11, 36399−36408

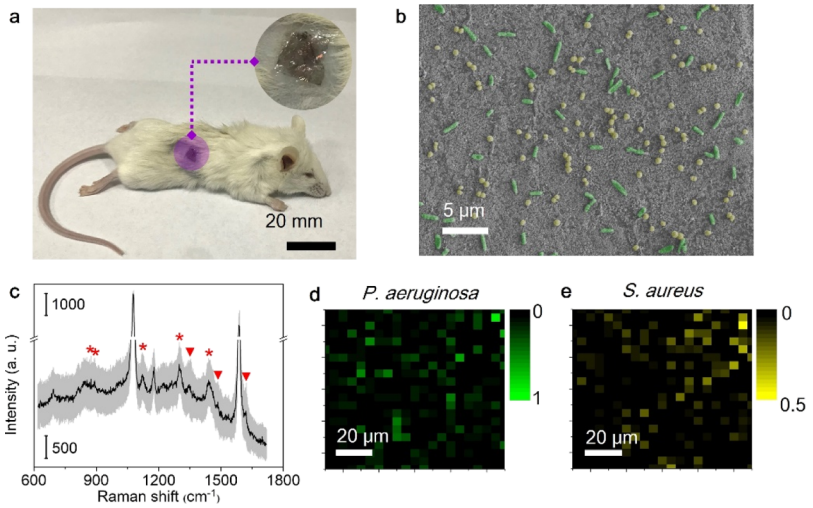

Figure 5. Sampling, release, and detection of *P. aeruginosa* and *S. aureus* from skin burn wound. (a) Optical images of SERS adhesive tape for sampling from mouse skin burn wound. (b) SEM image of *P. aeruginosa* (green) and *S. aureus* (yellow) sampled on tape (a). (c) Typical SERS spectra of adhesive tape (a) after 8 h of growth and (d,e) corresponding SERS imaging. The light gray region indicates the SD (n = 60). The red inverted triangles and asterisks indicate the characteristic SERS peaks of *P. aeruginosa* and *S. aureus*, respectively. Excitation laser: 785 nm; laser power: 4.5 mW; and exposure time: 10 s for (c) and 1 s for (d,e).

limit of detection of 1.8 nM, indicating its high sensitivity (Figure S16). The total analytical time of about 4 h was much shorter than previous approaches such as FTIR,[34] electrochemical,[35] and SERS assay.[36] The rapid detection procedure could be attributed to the highly efficient release and the high sensitivity of the SERS adhesive tape. The *P. aeruginosa* distribution on the solid culture medium could also be obtained by the SERS imaging after IS calibration (Figure 3c), which demonstrated the necessary of photocontrolled release for pathogen growth (Figure 3d). UV irradiation for 2 min led to an obvious increase of pathogen number after 4 h growth (Figure S17). Moreover, the adhesive tape showed the capability of long-term physiological analysis of pathogens. It could continuously monitor *P. aeruginosa* up to 24 h (Figure S18), at which eight more SERS peaks were observed because of the presence of more secreted pyocyanin.

To demonstrate the practicability of the SERS adhesive tape, it was further applied in *S. aureus* analysis. The simple immersion in 1.0×10^8 cfu/mL *S. aureus* suspension for 5 min showed a surface loading density of 6.2×10^6 cm^{-2} on the tape, and the photocontrolled release efficiency was 71.3 ± 8.8% (Figure 4a–c). After a 4 h growth, the characteristic SERS signals of *S. aureus* were also observed at 735 (amide, glycosidic ring mode), 782 (pyrimidine ring breathing), 874 and 895 [$\rho(CH_2)$ and ν(COC) in-plane symmetric ring deformation], 1128 and 1298 (amide III), and 1439 cm^{-1} [$\delta(CH_2)$ scissoring], which originated from peptidoglycan on bacterial cell walls[37,38] (Figure 4d), and were quite different from the SERS signals of pyocyanin secreted from *P. aeruginosa*. Thus, it is possible to use the SERS adhesive tape as an integrated platform for sampling, release, and detection of these two kinds of wound infectious pathogens.

Sampling, Release, and Detection of Pathogens from Skin Burn Wound. To mimic the early stage of concurrent infection, a mixture of 1×10^6 cfu/mL of *P. aeruginosa* and *S. aureus* was spiked on a skin burn wound of mouse, and simultaneous sampling (Figure 5a,b), transfer/release for growth, and SERS detection of these pathogens were performed with the adhesive tape. After photocontrolled release to LB agar and 8 h growth, the specific SERS signals from *P. aeruginosa* at 1356, 1486, and 1622 cm^{-1} and *S. aureus* at 874, 895, 1128, 1298, and 1439 cm^{-1} occurred in the mean SERS spectrum (Figure 5c), which were similar to previous reports.[28,37,38] The respective distribution of *P. aeruginosa* and *S. aureus* on the solid culture medium could also be obtained by SERS imaging (Figure 5d,e). Considering the advantages of SERS in pathogen detection,[39,40] the multiple characteristic peaks could offer reliable label-free recognition of *P. aeruginosa* and *S. aureus* infection. Compared with the traditional approaches such as colony culture and PCR methods for detecting wound infection, the SERS adhesive tape-based "three-in-one" analysis greatly simplified the operation and shortened the analytical time (Figure S19), indicating its outstanding potential in real sample testing.

Compared to recently developed pathogen analysis based on dispersed nanoparticles[5,41,42] or rigid substrates,[9,43,44] the "three-in-one" adhesive tape not only simplified the operation procedure but also reduced the bacterial sampling time to about 5 min because of the high capture efficiency and thus realized convenient and rapid detection of infected skin wound. Furthermore, the pathogen growth on culture medium after sampling and transfer steps could amplify the pathogen SERS signals and avoid the background interference from the sampling environment. The proposed detection strategy facilitated the covering of wound dressing materials and avoided direct laser irradiation, thus benefiting wound healing.[45]

CONCLUSIONS

This work designs a photocontrolled SERS adhesive tape to develop a "three-in-one" platform for rapid sampling, release, and detection of wound infectious pathogens. The adhesive tape can easily be pasted on an infected surface to perform fast sampling, transfer, and photocontrolled release of pathogens for appropriate growth and SERS detection. The adhesive tape possesses high surface loading and capture efficiency of pathogens by short-term immersion or pasting because of the strong electrostatic interaction between the modified

DOI: 10.1021/acsami.9b12823
ACS Appl. Mater. Interfaces 2019, 11, 36399–36408

quaternary ammonium groups and pathogens, excellent photocontrolled release ability because of the presence of *o*-nitrobenzyl moiety in the designed modification molecule, and good biocompatibility for retaining the reproduction activity of the released pathogens. The highly efficient release of pathogens and the high sensitivity of the SERS adhesive tape make it possible to detect the pathogens at an early growth stage and thus greatly shorten the analytical time. The integrated platform has been successfully used for simultaneous detection of *P. aeruginosa* and *S. aureus* on the skin burn wound of a mouse. The simple and convenient operation indicates promising practicability of the SERS adhesive tape in rapid detection of bacterial infection.

■ ASSOCIATED CONTENT

Supporting Information

The Supporting Information is available free of charge on the ACS Publications website at DOI: 10.1021/acsami.9b12823.

Characterization of PC molecule, control molecule, and AuNSs; uniformity and stability of SERS signals; contact angles of SERS tape without PC molecule modification; SERS spectra of SERS tape without and with PC molecule modification; confocal fluorescence images of SYTO 9-stained *P. aeruginosa* on SERS adhesive tapes modified with different concentrations of PC molecule; viability of captured and released pathogens; pathogen release efficiency on control SERS adhesive tape; pathogen detection at different growth times; quantitative response to spiked pyocyanin; live *P. aeruginosa* number under sampled SERS adhesive tapes; SERS detection of *P. aeruginosa* with 24 h growth; and comparison of pathogen detection procedures (PDF)

■ AUTHOR INFORMATION

Corresponding Authors

*E-mail: yingliu@nju.edu.cn (Y.L.).
*E-mail: wangry@nju.edu.cn (R.W.).
*E-mail: hxju@nju.edu.cn (H.J.).

ORCID

Ying Liu: 0000-0001-5718-7804
Huangxian Ju: 0000-0002-6741-5302

Notes

The authors declare no competing financial interest.

■ ACKNOWLEDGMENTS

This work was financially supported by the National Natural Science Foundation of China (21635005, 21605083, 41730316, 21827812, and 21890741) and the Natural Science Foundation of Jiangsu Province (BK 20160644). Specially appointed Professor Foundation of Jiangsu Province and Program for Innovative Talents and Entrepreneurs of Jiangsu Province.

■ REFERENCES

(1) Jones, K. E.; Patel, N. G.; Levy, M. A.; Storeygard, A.; Balk, D.; Gittleman, J. L.; Daszak, P. Global Trends in Emerging Infectious Diseases. *Nature* **2008**, *451*, 990−993.

(2) Grzybowski, J.; Janiak, M. K.; Oidak, E.; Lasocki, K.; Wrembel-Wargocka, J.; Cheda, A.; Antos-Bielska, M.; Pojda, Z. New Cytokine Dressings. II. Stimulation of Oxidative Burst in Leucocytes in vitro and Reduction of Viable Bacteria within an Infected Wound. *Int. J. Pharm.* **1999**, *184*, 179−187.

(3) Reisner, B. S.; Woods, G. L. Times to Detection of Bacteria and Yeasts in BACTEC 9240 Blood Culture Bottles. *J. Clin. Microbiol.* **1999**, *37*, 2024−2026.

(4) Chu, H.; Huang, Y. W.; Zhao, Y. P. Silver Nanorod Arrays as a Surface-Enhanced Raman Scattering Substrate for Foodborne Pathogenic Bacteria Detection. *Appl. Spectrosc.* **2008**, *62*, 922−931.

(5) Kearns, H.; Goodacre, R.; Jamieson, L. E.; Graham, D.; Faulds, K. SERS Detection of Multiple Antimicrobial-Resistant Pathogens Using Nanosensors. *Anal. Chem.* **2017**, *89*, 12666−12673.

(6) Zhang, L.; Xu, J. J.; Mi, L.; Gong, H.; Jiang, S. Y.; Yu, Q. M. Multifunctional Magnetic-Plasmonic Nanoparticles for Fast Concentration and Sensitive Detection of Bacteria using SERS. *Biosens. Bioelectron.* **2012**, *31*, 130−136.

(7) Malic, L.; Zhang, X.; Brassard, D.; Clime, L.; Daoud, J.; Luebbert, C.; Barrere, V.; Boutin, A.; Bidawid, S.; Farber, J.; Corneau, N.; Veres, T. Polymer-Based Microfluidic Chip for Rapid and Efficient Immunomagnetic Capture and Release of Listeria Monocytogenes. *Lab Chip* **2015**, *15*, 3994−4007.

(8) Verbarg, J.; Plath, W. D.; Shriver-Lake, L. C.; Howell, P. B.; Erickson, J. S., Jr.; Golden, J. P.; Ligler, F. S. Catch and Release: Integrated System for Multiplexed Detection of Bacteria. *Anal. Chem.* **2013**, *85*, 4944−4950.

(9) Wang, H.; Zhou, Y.; Jiang, X.; Sun, B.; Zhu, Y.; Wang, H.; Su, Y.; He, Y. Simultaneous Capture, Detection, and Inactivation of Bacteria as Enabled by a Surface-Enhanced Raman Scattering Multifunctional Chip. *Angew. Chem., Int. Ed.* **2015**, *54*, 5132−5136.

(10) Zhan, W.; Wei, T.; Cao, L.; Hu, C.; Qu, Y.; Yu, Q.; Chen, H. Supramolecular Platform with Switchable Multivalent Affinity: Photo-Reversible Capture and Release of Bacteria. *ACS Appl. Mater. Interfaces* **2017**, *9*, 3505−3513.

(11) Qu, Y.; Wei, T.; Zhan, W.; Hu, C.; Cao, L.; Yu, Q.; Chen, H. A Reusable Supramolecular Platform for the Specific Capture and Release of Proteins and Bacteria. *J. Mater. Chem. B* **2017**, *5*, 444−453.

(12) Wei, T.; Zhan, W.; Yu, Q.; Chen, H. Smart Biointerface with Photoswitched Functions between Bactericidal Activity and Bacteria-Releasing Ability. *ACS Appl. Mater. Interfaces* **2017**, *9*, 25767−25774.

(13) Akasaka, T.; Watari, F. Capture of Bacteria by Flexible Carbon Nanotubes. *Acta Biomater.* **2009**, *5*, 607−612.

(14) Shafiee, H.; Asghar, W.; Inci, F.; Yuksekkaya, M.; Jahangir, M.; Zhang, M. H.; Durmus, N. G.; Gurkan, U. A.; Kuritzkes, D. R.; Demirci, U. Paper and Flexible Substrates as Materials for Biosensing Platforms to Detect Multiple Biotargets. *Sci. Rep.* **2015**, *5*, 8719.

(15) Hills, K. D.; Oliveira, D. A.; Cavallaro, N. D.; Gomes, C. L.; McLamore, E. S. Actuation of Chitosan-Aptamer Nanobrush Borders for Pathogen Sensing. *Analyst* **2018**, *143*, 1650−1661.

(16) Xu, W.; Paidi, S. K.; Qin, Z.; Huang, Q.; Yu, C.-H.; Pagaduan, J. V.; Buehler, M. J.; Barman, I.; Gracias, D. H. Self-Folding Hybrid Graphene Skin for 3D Biosensing. *Nano Lett.* **2019**, *19*, 1409−1417.

(17) Xu, W.; Ling, X.; Xiao, J.; Dresselhaus, M. S.; Kong, J.; Xu, H.; Liu, Z.; Zhang, J. Surface Enhanced Raman Spectroscopy on a Flat Graphene Surface. *Proc. Natl. Acad. Sci. U.S.A.* **2012**, *109*, 9281−9286.

(18) Shiigi, H.; Fukuda, M.; Tono, T.; Takada, K.; Okada, T.; Dung, L. Q.; Hatsuoka, Y.; Kinoshita, T.; Takai, M.; Tokonami, S.; Nakao, H.; Nishino, T.; Yamamoto, Y.; Nagaoka, T. Construction of Nanoantennas on the Bacterial Outer Membrane. *Chem. Commun.* **2014**, *50*, 6252−6255.

(19) Shiigi, H.; Kinoshita, T.; Fukuda, M.; Le, D. Q.; Nishino, T.; Nagaoka, T. Nanoantennas as Biomarkers for Bacterial Detection. *Anal. Chem.* **2015**, *87*, 4042−4046.

(20) Guo, J.; Liu, Y.; Chen, Y.; Li, J.; Ju, H. A Multifunctional SERS Sticky Note for Real-Time Quorum Sensing Tracing and Inactivation of Bacterial Biofilms. *Chem. Sci.* **2018**, *9*, 5906−5911.

(21) Guo, J.; Chen, Y.; Li, J.; Liu, J.; Ju, H. A Self-Calibrated 2D Nanoarchitecture for Label-free SERS Quantitation and Distribution Imaging of Target. *Sens. Actuators, B* **2018**, *273*, 211−219.

(22) Hu, X.-L.; Chu, L. Y.; Dong, X. J.; Chen, G. R.; Tang, T. T.; Chen, D. J.; He, X. P.; Tian, H. Multivalent Glycosheets for Double Light-Driven Therapy of Multidrug-Resistant Bacteria on Wounds. *Adv. Funct. Mater.* **2019**, *29*, 1806986.

DOI: 10.1021/acsami.9b12823
ACS Appl. Mater. Interfaces 2019, 11, 36399−36408

(23) Veiga, A. S.; Schneider, J. P. Antimicrobial Hydrogels for the Treatment of Infection. *Biopolymers* **2013**, *100*, 637−644.
(24) Chen, S.; Wan, Q.; Badu-Tawiah, A. K. Mass Spectrometry for Paper-Based Immunoassays: Toward On-Demand Diagnosis. *J. Am. Chem. Soc.* **2016**, *138*, 6356−6359.
(25) Eisenführ, A.; Arora, P. S.; Sengle, G.; Takaoka, L. R.; Nowick, J. S.; Famulok, M. A ribozyme with michaelase activity. *Bioorg. Med. Chem.* **2003**, *11*, 235−249.
(26) Abdullahi, A.; Amini-Nik, S.; Jeschke, M. G. Animal Models in Burn Research. *Cell. Mol. Life Sci.* **2014**, *71*, 3241−3255.
(27) Dahiya, P. Burns as a Model of SIRS. *Front. Biosci.* **2009**, *14*, 4962−4967.
(28) Bodelón, G.; Montes-García, V.; López-Puente, V.; Hill, E. H.; Hamon, C.; Sanz-Ortiz, M. N.; Rodal-Cedeira, S.; Costas, C.; Celiksoy, S.; Pérez-Juste, I.; Scarabelli, L.; La Porta, A.; Pérez-Juste, J.; Pastoriza-Santos, I.; Liz-Marzán, L. M. Detection and Imaging of Quorum Sensing in *Pseudomonas aeruginosa* Biofilm Communities by Surface-Enhanced Resonance Raman Scattering. *Nat. Mater.* **2016**, *15*, 1203−1211.
(29) Ferrari, A. C.; Meyer, J. C.; Scardaci, V.; Casiraghi, C.; Lazzeri, M.; Mauri, F.; Piscanec, S.; Jiang, D.; Novoselov, K. S.; Roth, S.; Geim, A. K. Raman Spectrum of Graphene and Graphene Layers. *Phys. Rev. Lett.* **2006**, *97*, 187401.
(30) Kwon, Y. J.; Son, D. H.; Ahn, S. J.; Kim, M. S.; Kim, K. Vibrational Spectroscopic Investigation of Benzoic Acid Adsorbed on Silver. *J. Phys. Chem.* **1994**, *98*, 8481−8487.
(31) Joo, S. W.; Han, S. W.; Kim, K. Adsorption of 1,4-Benzenedithiol on Gold and Silver Surfaces: Surface-Enhanced Raman Scattering Study. *J. Colloid Interface Sci.* **2001**, *240*, 391−399.
(32) Chen, Q.; Yan, H.-J.; Yan, C.-J.; Pan, G.-B.; Wan, L.-J.; Wen, G.-Y.; Zhang, D.-Q. STM investigation of the dependence of alkane and alkane (C18H38, C19H40) derivatives self-assembly on molecular chemical structure on HOPG surface. *Surf. Sci.* **2008**, *602*, 1256−1266.
(33) Howard, M. D.; Jay, M.; Dziubla, T. D.; Lu, X. PEGylation of Nanocarrier Drug Delivery Systems: State of the Art. *J. Biomed. Nanotechnol.* **2008**, *4*, 133−148.
(34) Lasch, P.; Stämmler, M.; Zhang, M.; Baranska, M.; Bosch, A.; Majzner, K. FT-IR Hyperspectral Imaging and Artificial Neural Network Analysis for Identification of Pathogenic Bacteria. *Anal. Chem.* **2018**, *90*, 8896−8904.
(35) Kim, E.; Gordonov, T.; Bentley, W. E.; Payne, G. F. Amplified and in Situ Detection of Redox-Active Metabolite Using a Biobased Redox Capacitor. *Anal. Chem.* **2013**, *85*, 2102−2108.
(36) Wu, X.; Chen, J.; Li, X.; Zhao, Y.; Zughaier, S. M. Culture-Free Diagnostics of *Pseudomonas aeruginosa* Infection by Silver Nanorod Array based SERS from Clinical Sputum Samples. *Nanomedicine* **2014**, *10*, 1863−1870.
(37) Williams, A. C.; Edwards, H. G. M. Fourier Transform Raman Spectroscopy of Bacterial Cell Walls. *J. Raman Spectrosc.* **1994**, *25*, 673−677.
(38) Ayala, O. D.; Wakeman, C. A.; Pence, I. J.; Gaddy, J. A.; Slaughter, J. C.; Skaar, E. P.; Mahadevan-Jansen, A. Drug-Resistant *Staphylococcus aureus* Strains Reveal Distinct Biochemical Features with Raman Microspectroscopy. *ACS Infect. Dis.* **2018**, *4*, 1197−1210.
(39) Premasiri, W. R.; Moir, D. T.; Klempner, M. S.; Krieger, N.; Jones, G., II; Ziegler, L. D. Characterization of the Surface Enhanced Raman Scattering (SERS) of Bacteria. *J. Phys. Chem. B* **2005**, *109*, 312−320.
(40) Chen, Y.; Premasiri, W. R.; Ziegler, L. D. Surface Enhanced Raman Spectroscopy of *Chlamydia trachomatis* and *Neisseria gonorrhoeae* for Diagnostics, and Extra-Cellular Metabolomics and Biochemical Monitoring. *Sci. Rep.* **2018**, *8*, 5163.
(41) Zhou, H.; Yang, D.; Ivleva, N. P.; Mircescu, N. E.; Schubert, S.; Niessner, R.; Wieser, A.; Haisch, C. Label-Free in Situ Discrimination of Live and Dead Bacteria by Surface-Enhanced Raman Scattering. *Anal. Chem.* **2015**, *87*, 6553−6561.
(42) Mühlig, A.; Bocklitz, T.; Labugger, I.; Dees, S.; Henk, S.; Richter, E.; Andres, S.; Merker, M.; Stöckel, S.; Weber, K.; Cialla-May, D.; Popp, J. LOC-SERS: A Promising Closed System for the Identification of Mycobacteria. *Anal. Chem.* **2016**, *88*, 7998−8004.
(43) Cao, Y.; Lv, M.; Xu, H.; Svec, F.; Tan, T.; Lv, Y. Planar Monolithic Porous Polymer Layers Functionalized with Gold Nanoparticles as Large-Area Substrates for Sensitive Surface-Enhanced Raman Scattering Sensing of Bacteria. *Anal. Chim. Acta* **2015**, *896*, 111−119.
(44) Liu, T.-Y.; Tsai, K.-T.; Wang, H.-H.; Chen, Y.; Chen, Y.-H.; Chao, Y.-C.; Chang, H.-H.; Lin, C.-H.; Wang, J.-K.; Wang, Y.-L. Functionalized Arrays of Raman-Enhancing Nanoparticles for Capture and Culture-Free Analysis of Bacteria in Human Blood. *Nat. Commun.* **2011**, *2*, 538.
(45) Fan, Z.; Liu, B.; Wang, J.; Zhang, S.; Lin, Q.; Gong, P.; Ma, L.; Yang, S. A Novel Wound Dressing Based on Ag/Graphene Polymer Hydrogel: Effectively Kill Bacteria and Accelerate Wound Healing. *Adv. Funct. Mater.* **2014**, *24*, 3933−3943.

DOI: 10.1021/acsami.9b12823
ACS Appl. Mater. Interfaces 2019, 11, 36399−36408